

## RESEARCH PAPER

# Endothelin-1 suppresses insulin-stimulated Akt phosphorylation and glucose uptake via GPCR kinase 2 in skeletal muscle cells

### Correspondence

Takahiro Horinouchi, Department of Cellular Pharmacology, Hokkaido University Graduate School of Medicine, North 15, West 7, Sapporo City, Hokkaido 060-8638, Japan.  
E-mail: horinouc@med.hokudai.ac.jp

### Received

30 October 2014

### Revised

24 November 2015

### Accepted

3 December 2015

Takahiro Horinouchi, Akimasa Hoshi, Takuya Harada, Tsunaki Higa, Sarita Karki, Koji Terada, Tsunehito Higashi, Yosuke Mai, Prabha Nepal, Yuichi Mazaki and Soichi Miwa

*Department of Cellular Pharmacology, Hokkaido University Graduate School of Medicine, Sapporo City, Japan*

## BACKGROUND AND PURPOSE

Endothelin-1 (ET-1) reduces insulin-stimulated glucose uptake in skeletal muscle, inducing insulin resistance. Here, we have determined the molecular mechanisms underlying negative regulation by ET-1 of insulin signalling.

## EXPERIMENTAL APPROACH

We used the rat L6 skeletal muscle cells fully differentiated into myotubes. Changes in the phosphorylation of Akt was assessed by Western blotting. Effects of ET-1 on insulin-stimulated glucose uptake was assessed with [<sup>3</sup>H]-2-deoxy-D-glucose ([<sup>3</sup>H]2-DG). The C-terminus region of GPCR kinase 2 (GRK2-ct), a dominant negative GRK2, was overexpressed in L6 cells using adenovirus-mediated gene transfer. GRK2 expression was suppressed by transfection of the corresponding short-interfering RNA (siRNA).

## KEY RESULTS

In L6 myotubes, insulin elicited sustained Akt phosphorylation at Thr<sup>308</sup> and Ser<sup>473</sup>, which was suppressed by ET-1. The inhibitory effects of ET-1 were prevented by treatment with a selective ET<sub>A</sub> receptor antagonist and a G<sub>q</sub> protein inhibitor, overexpression of GRK2-ct and knockdown of GRK2. Insulin increased [<sup>3</sup>H]2-DG uptake rate in a concentration-dependent manner. ET-1 noncompetitively antagonized insulin-stimulated [<sup>3</sup>H]2-DG uptake. Blockade of ET<sub>A</sub> receptors, overexpression of GRK2-ct and knockdown of GRK2 prevented the ET-1-induced suppression of insulin-stimulated [<sup>3</sup>H]2-DG uptake. In L6 myotubes overexpressing FLAG-tagged GRK2, ET-1 facilitated the interaction of endogenous Akt with FLAG-GRK2.

## CONCLUSIONS AND IMPLICATIONS

Activation of ET<sub>A</sub> receptors with ET-1 suppressed insulin-induced Akt phosphorylation at Thr<sup>308</sup> and Ser<sup>473</sup> and [<sup>3</sup>H]2-DG uptake in a GRK2-dependent manner in skeletal muscle cells. These findings suggest that ET<sub>A</sub> receptors and GRK2 are potential targets for overcoming insulin resistance.

## Abbreviations

ET-1, endothelin-1; FCS, fetal calf serum; GLUT, glucose transporter; GRK2, GPCR kinase 2; GRK2-ct, C-terminus region of GPCR kinase 2; [<sup>3</sup>H]2-DG, [1,2-<sup>3</sup>H(N)]-2-deoxy-D-glucose; HRP, horseradish peroxidase; HS, horse serum; InsR, insulin receptor; IRS, insulin receptor substrate; PTX, *Pertussis* toxin; siRNA, short interfering RNA

## Tables of Links

TARGETS
<b>GPCRs<sup>a</sup></b>
ETA receptor
ETB receptor
<b>Catalytic receptors<sup>b</sup></b>
InsR, insulin receptor
<b>Transporters<sup>c</sup></b>
GLUT4, SLC2A4
<b>Enzymes<sup>d</sup></b>
Akt
GRK2, GPCR kinase 2 (BARK1)

LIGANDS
2-DG, 2-deoxy-d-glucose
BQ-123
BQ-788
ET-1, endothelin 1
Insulin
LY294002
NF449

These Tables list key protein targets and ligands in this article which are hyperlinked to corresponding entries in <http://www.guidetopharmacology.org>, the common portal for data from the IUPHAR/BPS Guide to PHARMACOLOGY (Pawson *et al.*, 2014) and are permanently archived in the Concise Guide to PHARMACOLOGY 2015/16 (<sup>a,b,c,d</sup>Alexander *et al.*, 2015a,b,c,d).

## Introduction

Endothelin-1 (ET-1) is a potent vasoconstrictor and pro-inflammatory peptide (Yanagisawa *et al.*, 1988), which has been implicated in the pathophysiology of various diseases, including diabetes mellitus (Pernow *et al.*, 2012), systemic and pulmonary hypertension (Rodríguez-Pascual *et al.*, 2011) and atherosclerosis (Pernow *et al.*, 2012). Plasma levels of ET-1 are elevated in patients with these diseases (Ferri *et al.*, 1995; Lerman *et al.*, 1991; Takahashi *et al.*, 1990; Touyz and Schiffrin, 2003). Excessive production of ET-1 causes a prolonged vasoconstriction mediated mainly through ET<sub>A</sub> receptors (Horinouchi *et al.*, 2013), endothelial dysfunction resulting from down-regulation of ET<sub>B</sub> receptors (Rubin, 2012) and insulin resistance (Shemyakin *et al.*, 2011; Usui *et al.*, 2005).

Insulin resistance is a condition where the sensitivity to insulin of the cells expressing insulin receptors (InsR) is decreased because of a functional disturbance of insulin-mediated intracellular signalling. The most important tissue involved in the lowering of blood glucose levels by insulin is skeletal muscle, accounting for approximately 70% of total glucose uptake in healthy subjects (DeFronzo, 1988). Accordingly, disturbance of insulin-stimulated glucose uptake into skeletal muscle is mainly responsible for elevated blood glucose levels in patients with type 2 diabetes (DeFronzo, 1988), where there is no significant change in glucose transporter 4 (GLUT4) protein levels (Schalin-Jäntti *et al.*, 1994).

Insulin increases glucose uptake in skeletal muscle cells through facilitating translocation of GLUT4 from intracellular storage vesicles to the plasma membrane, as detailed below and reviewed by Leto and Saltiel (2012). Activation of InsRs induces phosphorylation of the corresponding substrate protein (IRS), resulting in the recruitment and activation of PI3K. PI3K converts phosphatidylinositol-4,5-diphosphate to phosphatidylinositol-3,4,5-trisphosphate, which is involved

in the recruitment of phosphoinositide-dependent kinase 1 and Akt (Shisheva, 2008). Akt translocated to the plasma membrane is activated by phosphorylation at Thr<sup>308</sup> by phosphoinositide-dependent kinase 1 and at Ser<sup>473</sup> by mammalian target of rapamycin complex 2 (Laplante and Sabatini, 2012; Sarbassov *et al.*, 2005). Activated Akt facilitates the translocation of GLUT4 to the plasma membrane by phosphorylation and subsequent inactivation of the Rab-GTPase-activating protein, AS160. The decreased Rab-GTPase activity increases the ratio of the GTP-bound form (active form) of Rab to the GDP-bound form (inactive form), leading to facilitation of GLUT4 translocation and cell membrane fusion. This sequence of events demonstrate that Akt activation is essential for insulin-stimulated glucose uptake via GLUT4 in skeletal muscle.

Several studies have suggested that ET-1 induces insulin resistance through a direct action on skeletal muscle, rather than reduced insulin delivery to the skeletal muscle resulting from vasoconstriction. In healthy subjects, administration of exogenous ET-1 reduces insulin-stimulated glucose uptake in skeletal muscle without decreasing skeletal muscle blood flow (Ottosson-Seeberger *et al.*, 1997). In addition, prolonged treatment of primary culture of human skeletal muscle cells with ET-1 impairs insulin-stimulated Akt phosphorylation and glucose uptake (Shemyakin *et al.*, 2011). However, the signalling pathways underlying the inhibitory effects of ET-1 on the insulin-induced facilitation of Akt phosphorylation and glucose uptake in skeletal muscle cells are not yet known.

Growing evidence shows that the GPCR kinase 2 (GRK2), a ubiquitous Ser/Thr protein kinase, can function as a negative regulator of insulin signalling in a phosphorylation-independent manner, although it was originally identified as a kinase, which specifically phosphorylates and desensitizes agonist-stimulated GPCRs (Evron *et al.*, 2012). Several lines of evidence demonstrate that GRK2 binds to a range of signalling molecules including Akt (Liu *et al.*, 2005) and G<sub>βγ</sub>

subunits (Evron *et al.*, 2012). A direct interaction of GRK2 with Akt impairs Akt activation, causing negative regulation of Akt signalling (Liu *et al.*, 2005). Binding of GRK2 to  $G_{\beta\gamma}$  subunits is essential for translocation of GRK2 to the plasma membrane (Evron *et al.*, 2012). These data encouraged us to assume that activation of ET receptors in skeletal muscle cells induced insulin resistance through inhibition of Akt signalling, namely, activation of ET receptors promoted dissociation of receptor-coupled G protein into its subunits,  $G_{\alpha}$  and  $G_{\beta\gamma}$ ; the increase in the local concentration of  $G_{\beta\gamma}$  subunit in turn recruited GRK2 to the plasma membrane, leading to the augmented interaction of GRK2 with Akt at the plasma membrane and the resulting inhibition of Akt signalling.

The purpose of this study was to determine molecular mechanisms underlying negative regulation by ET-1 of insulin signalling in rat L6 myotubes, with particular attention to the possible involvement of GRK2. Because both GLUT4 protein and insulin-stimulated glucose uptake via GLUT4 were increased during myogenesis in L6 cells (Mitsumoto and Klip, 1992), L6 myoblasts were highly differentiated into myotubes with a modified method to estimate insulin-stimulated glucose uptake.

## Methods

### Construction of retrovirus vector

The pcDNA3 mammalian expression vector encoding FLAG-tagged GRK2 (FLAG-GRK2) was generously provided by Dr. Hitoshi Kurose (Kyusyu University, Fukuoka, Japan). The vector was digested with two restriction enzymes (BamHI and NotI) simultaneously to obtain the insert cDNA of FLAG-GRK2. The cDNA fragment was ligated into the BamHI/NotI-treated pMXrmv5 retrovirus vector to yield the pMXrmv5 vectors encoding FLAG-GRK2.

### Cell culture

Rat L6 skeletal muscle cell line was obtained from the Health Science Research Resources Bank (Osaka, Japan) and cultured in low-glucose DMEM supplemented with 5% (v.v<sup>-1</sup>) fetal calf serum (FCS), penicillin (100 units·mL<sup>-1</sup>) and streptomycin (100 µg·mL<sup>-1</sup>) at 37°C in humidified air with 5% CO<sub>2</sub>. For differentiation of myoblasts into myotubes, myoblasts were seeded into six-well plates at a density of approximately 10<sup>6</sup> cells per well and cultured in low-glucose DMEM supplemented with 5% FCS for 2 days. To induce differentiation, the cells were maintained in low-glucose DMEM supplemented with 2% horse serum (HS) and 10 µg·mL<sup>-1</sup> human insulin for 7 days with medium change every 2 days (Figure 1A). For Western blot analysis and [<sup>3</sup>H]2-DG uptake assay, the differentiated myotubes (Day 7) were serum starved in low-glucose DMEM for 2 or 3 days with daily medium change prior to performing the examination (unless indicated otherwise).

### Stable expression of FLAG-GRK2 in L6 cells

To generate L6 cells stably expressing FLAG-GRK2, the gene was introduced into L6 myoblasts by retroviral gene transfer as described previously (Horinouchi *et al.*, 2012).

### Adenovirus infection

Recombinant adenoviruses encoding GFP and the carboxyl terminal region of GRK2 (GRK2-ct) were kindly provided by Dr. Hitoshi Kurose (Kyusyu University). L6 myotubes (Day 7) maintained in six-well plates were infected by recombinant adenoviruses encoding GFP or GRK2-ct for 2 h. After infection, the cells were cultured in low-glucose DMEM containing 2% HS for 12 h. Subsequently, L6 myotubes were cultured in serum-free, low-glucose DMEM for 2 days for Western blot analysis or 3 days for assay of [<sup>3</sup>H]-2-deoxy-D-glucose ([<sup>3</sup>H]2-DG) uptake.

### Transfection of siRNA

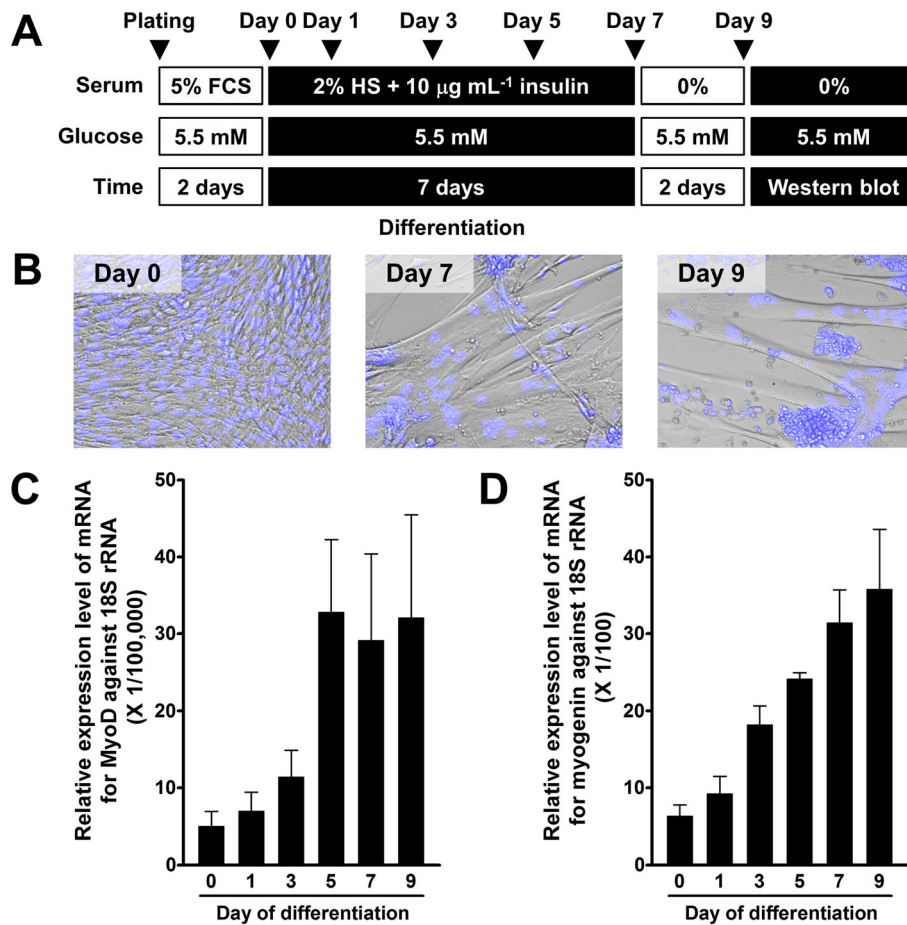
Control and GRK2 siRNAs were transfected into L6 myotubes (Day 6) maintained in six-well plates using Lipofectamine RNAiMAX Transfection Reagent according to the manufacturer's protocol with minor modifications. Briefly, 40 pmol of siRNA was diluted in 0.5 mL of Opti-MEM I without serum. The Lipofectamine RNAiMAX Transfection Reagent (7.5 µL) was diluted in the diluted siRNA solution, and the mixture was incubated at room temperature for 20 min. Cell culture medium was removed from wells of six-well plates, and the mixture of siRNA and Lipofectamine RNAiMAX Transfection Reagent was added to each well. Then, 0.5 mL of low-glucose DMEM containing 0.5% FCS was added to the well without removing the transfection mixture, and the cells were incubated for 72 h. During 72 h incubation, 0.5 mL of low-glucose DMEM was added to each well every 24 h without removing the transfection mixture. For Western blot analysis and assay of [<sup>3</sup>H]2-DG uptake, the cells were serum starved in low-glucose DMEM for 24 h prior to performing the experiments.

### Visualization of cell nuclei and imaging of spontaneously contracting myotubes

L6 myoblasts (Day 0) and myotubes (Days 7 and 9) were incubated with a DNA-specific fluorescent dye, Hoechst 33342 (1 µg·mL<sup>-1</sup>), for 30 min in culture medium at 37°C in humidified air with 5% CO<sub>2</sub>. The fluorescent images for Hoechst 33342 and the phase contrast images were obtained using a fluorescence microscopy (IX-71, Olympus Corp., Tokyo, Japan) equipped with ×20 objective lens (LUCPLFLN, NA = 0.45, Olympus).

### Measurement of mRNA expression levels for MyoD, myogenin, and 18S rRNA by quantitative RT-PCR

Total RNA of L6 cells was extracted at indicated days (Figure 1C and D) and purified by using total RNA purification kit (RNeasy Mini Kit, QIAGEN, Tokyo, Japan) following the manufacturer's instructions. Quantitative RT-PCR was performed by using both SuperScript III First-Strand Synthesis System (Thermo Fisher Scientific Inc.) for RT and FastStart Essential DNA Green Master kit (Roche Diagnostics GmbH, Mannheim, Germany) with gene-specific primers for quantitative PCR (Table 1). Synthesized cDNA was heated for 10 min at 95°C and then amplified by 45 cycles (95°C for 10 s, 60°C for 10 s and 72°C for 15 s) using a programmable thermal cycler (LightCycler Nano; Roche Diagnostics GmbH). The PCR

**Figure 1**

Differentiation of L6 myoblasts into myotubes. (A) Protocol for differentiation of L6 myoblasts into myotubes. (B) Phase contrast images of undifferentiated myoblasts (Day 0) and differentiated myotubes (Days 7 and 9) obtained at the same magnification. The nucleus was stained with Hoechst 33342 dye as shown in blue. (C and D) Changes in mRNA levels of differentiation marker genes, MyoD (C) and myogenin (D), during differentiation. Ordinate represents relative expression levels against 18S rRNA as an internal control gene. Data are presented as means  $\pm$  SEM of the results obtained from five experiments.

**Table 1**

Oligonucleotides used as PCR primers

Gene	Forward Primer (5' to 3')	Reverse Primer (5' to 3')	Product size (bp)	References
Rat MyoD	GGAGACATCTCAAGCGATGC	AGCACCTGGTAAATCGGATTG	105	(Gomes <i>et al.</i> , 2006)
Rat myogenin	ACTACCCACCGTCCATTAC	TCGGGGCACTCACTGTCTCT	233	(Kamikawa <i>et al.</i> , 2013)
Rat 18S rRNA	CACGGGTGACGGGAATCAG	CGGGTCCGGAGTGGGTAATTTG	105	(Kim <i>et al.</i> , 2011)
Rat ET <sub>A</sub> receptor	ATGGGTGTCCTTTGCTTTCTGGCGT	TTAGTTCATGCTGTCCTTGTTGGCTG	1281	–
Rat C <sub>q</sub> protein	ATGACTCTGGAGTCCATCATGGCGT	TTAGACCAGATTGTACTCCTTCAGG	1080	–
Rat G <sub>11</sub> protein	ATGACTCTGGAGTCCATGATAGCGT	TCAGACCAGTTGTACTCCTTCAGG	1080	–
Rat GRK2-ct	GCCAAAAACAACAGCTGGGC	ACTGCCACGCTGAATCAGTGG	432	–
Rat InsR	CAGGATTGGCGCTGTGTAAC	CACAGCTGCCTCAGGTTCTG	491	(Obici <i>et al.</i> , 2002)
Rat Akt2	ATGAATGAGGTATCTGTCATCAAAG	TCACTCTCGGATGCTGGCTGAGTAG	1446	–
Rat GLUT4	ATGCCGTCGGGTTTCCAGCAGATCGGC	TCAGTCATTCTCATCTGGCCCTAAGTATTC	1530	–

products were confirmed by a single band on electrophoresis and by the single melting temperature. The 18S rRNA gene was used as an internal control for normalization of the data. Expression levels of mRNAs for MyoD and myogenin were represented as a ratio to 18S rRNA.

### Western blot analysis

Western blot analysis was carried out as described previously (Harada *et al.*, 2014). The primary antibodies [phospho-Akt (Thr<sup>308</sup>), phospho-Akt (Ser<sup>473</sup>), total Akt (pan), phospho-ERK1/2, total-ERK1/2 and IRS-1] bound to proteins on membranes were detected with a secondary HRP-conjugated anti-rabbit IgG antibody and Pierce Western blotting Substrate (Thermo Fisher Scientific Inc.). The blots were exposed to Amersham Hyperfilm ECL (GE Healthcare Ltd., Little Chalfont, Buckinghamshire, UK). OD on the film was analysed with National Institutes of Health Image J1.37 software. The phosphorylation levels of Akt at Thr<sup>308</sup> and Ser<sup>473</sup> were routinely expressed as the ratio of phosphorylated Akt to total Akt. Akt phosphorylation responses were normalized to the level of insulin-stimulated Akt phosphorylation in L6 myotubes without treatment with ET-1, vehicle, antagonist, inhibitor, adenovirus or siRNA.

### Co-immunoprecipitation assay

Co-immunoprecipitation experiment and subsequent Western blot analysis were carried out as described previously (Horinouchi *et al.*, 2012). The primary antibody [total Akt (pan) and IRS-1] bound to proteins on membranes was detected with Clean-Blot IP Detection Reagent HRP for immunoprecipitated samples or a secondary HRP-conjugated anti-rabbit IgG antibody for whole cell lysates. The Clean-Blot reagent and HRP-conjugated antibody were detected with ImmunoStar LD (Wako Pure Chemical Industries, Ltd.) and Pierce Western blotting Substrate (Thermo Fisher Scientific Inc.), respectively. The membranes were then stripped with stripping buffer [62.5 mM Tris-HCl (pH 7.0), 2% SDS, 1% 2-mercaptoethanol] for 1 h at 50°C and reprobed with an anti-FLAG HRP antibody. The blots were exposed to Amersham Hyperfilm ECL (GE Healthcare Ltd.). The amounts of immunoprecipitated proteins were analysed with National Institutes of Health Image J1.37 software.

### [<sup>3</sup>H]2-DG uptake assay

L6 myotubes (Day 7) maintained in six-well plates were serum starved in low-glucose DMEM for 3 days (unless indicated otherwise) prior to performing [<sup>3</sup>H]2-DG uptake assay. The cells were incubated in serum-free DMEM supplemented with 1.0 mM D-glucose and 1.0 mM sodium pyruvate (assay medium) for 30 min before each experiment. To estimate insulin-stimulated [<sup>3</sup>H]2-DG uptake, the cells were treated with insulin and 100 nM [<sup>3</sup>H]2-DG in serum-free assay medium. [<sup>3</sup>H]2-DG uptake was terminated by rapid washing three times with 3 mL of PBS (37°C) containing 20.0 mM D-glucose. For quantitation of [<sup>3</sup>H]2-DG uptake, the cells were collected with 1.0 mL of 0.5 M NaOH (60°C) and completely digested with shaking at 150 rpm for 60 min at 60°C. The radioactivity in the lysate was counted in a liquid scintillation counter (LC-3500; Aloka, Tokyo, Japan) using a scintillation fluid (Clear-sol II; Nacalai Tesque

Inc., Kyoto, Japan). The protein content in the lysate was determined with the method of Bradford (1976) using BSA as standard.

### Data analysis

These studies comply with the recommendations on experimental design and analysis in pharmacology (Curtis *et al.*, 2015). The results are presented as means ± SEM, where *n* refers to the number of experiments. The significance of the difference between mean values was evaluated with GraphPad prism (version 3.00, GraphPad software Inc., San Diego, CA, USA) by unpaired *t*-test or one-way ANOVA followed by Tukey's multiple comparison test. A *P*-value less than 0.05 was considered to indicate significant differences.

### Materials

YM-254890 was kindly provided by Astellas Pharma Inc. (Tokyo, Japan). The following drugs and reagents were used in the present study: synthetic human ET-1, BQ-123 [cyclo (D-trp-D-asp-L-pro-D-val-L-leu)], BQ-788 (*N*-cis-2,6-dimethylpiperidinocarbonyl-L-γ-methylleucyl-D-1-methoxycarbonyltryptophanyl-D-norleucine) (Peptide Institute, Osaka, Japan); human insulin (Cell Science and Technology Institute, Inc., Miyagi, Japan); BSA, Hoechst 33342 (Sigma-Aldrich Co., St. Louis, MO, USA.); LY294002 [2-(4-morpholinyl)-8-phenyl-4*H*-1-benzopyran-4-one], Pertussis toxin (PTX) (Calbiochem, San Diego, CA, USA); [1,2-<sup>3</sup>H(N)]-2-deoxy-D-glucose ([<sup>3</sup>H]2-DG; specific activity: 8.0 Ci·mmol<sup>-1</sup>, 1.0 mCi·mL<sup>-1</sup> in aqueous solution, PerkinElmer, Inc., Boston, MA, USA); FCS, HS, D-glucose-free and sodium pyruvate-free DMEM, EDTA-free, protease inhibitor cocktail (Thermo Fisher Scientific Inc., Waltham, MA, USA); low-glucose (5.5 mM) DMEM (Wako Pure Chemical Industries, Ltd., Osaka, Japan); GSK2126458 [2,4-difluoro-*N*-(2-methoxy-5-(4-(pyridazin-4-yl)quinolin-6-yl)pyridin-3-yl)benzenesulfonamide] (Selleck Chemicals, Houston, TX, USA); NF449 (4,4',4'',4'''-[carbonylbis(imino-5,1,3-benzenetriyl-bis(carbonylimino))]tetrakis-1,3-benzenedisulfonic acid, octasodium salt) (Tocris Bioscience, Bristol, UK); ON-TARGETplus Rat Adrbk1 (25238) short-interfering RNA (siRNA) – SMARTpool (L-090990-02-0005), ON-TARGETplus non-targeting Pool (D-001810-10-05) (GE Healthcare Dharmacon Inc., Lafayette, CO, USA); and Lipofectamine RNAiMAX Transfection Reagent, Opti-MEM I Reduced Serum Medium (Thermo Fisher Scientific Inc.). Primary antibodies for phospho-Akt (Thr<sup>308</sup>), phospho-Akt (Ser<sup>473</sup>), total Akt (pan), phospho-ERK1/2 (Thr<sup>202</sup>/Tyr<sup>204</sup>), total ERK1/2, and IRS-1, and a secondary horseradish peroxidase (HRP)-conjugated anti-rabbit IgG antibody were obtained from Cell Signalling Technology Inc. (Beverly, MA, USA). Primary antibodies for FLAG peptide, HRP-conjugated FLAG peptide (HRP-FLAG) and GFP were obtained from Sigma-Aldrich, Medical and Biological Laboratories Co., Ltd. (Aichi, Japan) and Clontech Laboratories, Inc. (Mountain View, CA, U.S.A.) respectively. GRK2 antibody (C-15) and normal mouse IgG were obtained from Santa Cruz Biotechnology, Inc. (Dallas, TX, USA). Clean-Blot IP Detection Reagent HRP was obtained from Thermo Fisher Scientific Inc. The other reagents used were of analytical grade.

## Results

### Differentiation of mononucleated myoblasts into contractile, multinucleated myotubes

Figure 1B shows that mononucleated myoblasts (Day 0) are differentiated into multinucleated myotubes (Day 7) during culture in the differentiation medium. Some of the myotubes (Day 7) were able to constrict spontaneously (Supporting Information Movie S1). The myotubes (Day 7) were resistant to serum starvation for at least 3 days (Figure 1B, Day 9 after serum starvation for 2 days). Quantitative RT-PCR analysis has demonstrated that mRNA expression levels for differentiation marker genes, MyoD and

myogenin (Bentzinger *et al.*, 2012), are increased during differentiation for 9 days with a different time course (Figure 1C and D). The maximal mRNA expression level of MyoD was observed at Day 5 and was maintained for at least 4 days (Figure 1C). On the other hand, the mRNA expression level of myogenin was increased with time and reached its maximum at Day 9 (Figure 1D).

As shown in Supporting Information Fig. S1, the expression level of mRNA for ET<sub>A</sub> receptors was slightly but significantly decreased after differentiation. On the other hand, mRNA expression levels of GRK2 and GLUT4 were increased after differentiation. There was no statistically significant difference in mRNA expression levels of G<sub>q</sub> protein, G<sub>11</sub> protein, InsR and Akt2 between Day 0 and Day 7.

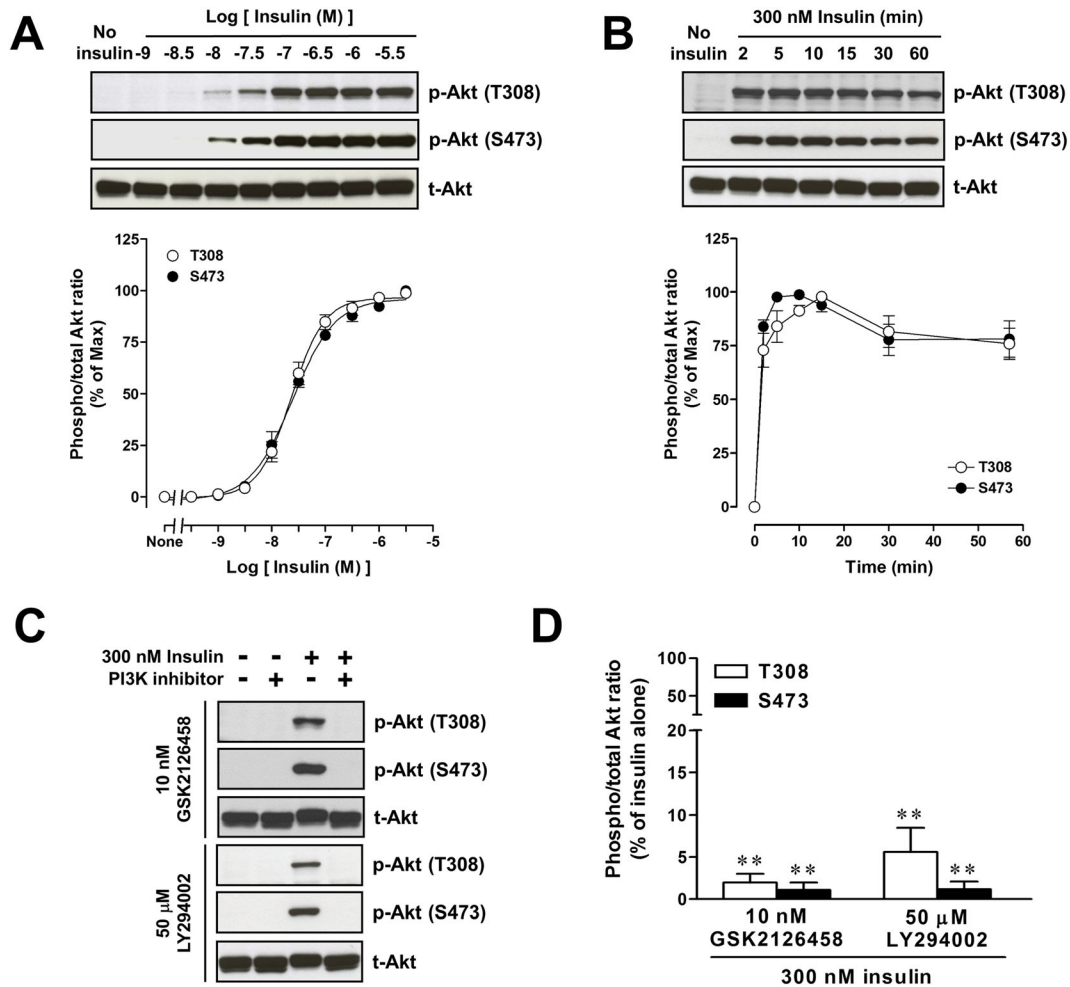


### Figure 2

Characterization of Akt phosphorylation in response to insulin in L6 myotubes. (A) Concentration-response curves for Akt phosphorylation in response to 5 min exposure to insulin with representative immunoblots using antibodies to phospho-Akt at Thr<sup>308</sup> [p-Akt (T308)], phospho-Akt at Ser<sup>473</sup> [p-Akt (S473)] and total Akt (t-Akt). (B) Time course of Akt phosphorylation induced by 300 nM insulin with representative immunoblots. (C and D) Effects of GSK2126458 and LY294002 on Akt phosphorylation in response to 5 min exposure to 300 nM insulin in L6 myotubes. The cells were treated with 10 nM GSK2126458 or 50 μM LY294002 for 30 min before stimulation with insulin. Representative immunoblots were obtained using antibodies to p-Akt (T308), p-Akt (S473) and t-Akt. (A and B) Ordinate represents Akt phosphorylation responses, which are normalized to the level of insulin-stimulated maximal Akt phosphorylation. (D) Ordinate represents Akt phosphorylation responses, which are normalized to the level of insulin-stimulated Akt phosphorylation in L6 myotubes without treatment with GSK2126458 or LY294002. Data are presented as means ± SEM of the results obtained from six experiments. When no error bar is shown, the error is smaller than the symbol. \*\*  $P < 0.01$  versus its control (300 nM insulin alone).

### Characterization of insulin-induced Akt phosphorylation in L6 myotubes

Treatment of L6 myotubes with insulin at concentrations ranging from 1 nM to 3  $\mu$ M for 5 min elicited phosphorylation of Akt at Thr<sup>308</sup> and Ser<sup>473</sup> in a concentration-dependent manner with pEC<sub>50</sub> values of  $7.59 \pm 0.08$  for Thr<sup>308</sup> and  $7.63 \pm 0.08$  for Ser<sup>473</sup> ( $n = 6$  for each) (Figure 2A). There was no difference in the pEC<sub>50</sub> values for phosphorylation of Thr<sup>308</sup> and Ser<sup>473</sup>. The phosphorylation of Akt induced by 300 nM insulin was increased rapidly after insulin stimulation and reached its maximal level at around 5 min and was kept at that level for up to 15 min. The level of phosphorylation declined slightly at 30 min and remained constant up to 60 min (Figure 2B). The Akt phosphorylation at Thr<sup>308</sup> and Ser<sup>473</sup> in response to stimulation with 300 nM insulin for 5 min was significantly inhibited by two PI3K inhibitors, GSK2126458 (Knight *et al.*, 2010) or LY294002 (Shepherd *et al.*, 1997) (Figure 2C and D).

### Effects of ET-1 on insulin-induced Akt phosphorylation in L6 myotubes

In the absence of insulin stimulation, treatment with 30 nM ET-1 for the corresponding times had no effect on basal levels of Akt phosphorylation (Supporting Information Fig. S2). Akt phosphorylation at Thr<sup>308</sup> and Ser<sup>473</sup> induced by 100 nM insulin stimulation for 60 min was inhibited by treatment with 30 nM ET-1, and increased with longer times of treatment. The maximal inhibition of around 50% was observed following ET-1 treatment for 10–15 min (Figure 3).

### Molecular mechanisms for ET-1-induced inhibition of insulin-stimulated Akt phosphorylation in L6 myotubes

In the presence of 0.1% DMSO (as a vehicle), treatment with ET-1 for 2 and 5 min inhibited phosphorylation of Akt at Thr<sup>308</sup> and Ser<sup>473</sup> induced by treatment with 100 nM insulin for 60 min (Figure 4). Notably, the inhibitory effects of ET-1 were blocked by treatment with 1  $\mu$ M BQ-123 (a selective ET<sub>A</sub> receptor antagonist) and 300 nM YM-254890 (a selective G<sub>q</sub> protein inhibitor). However, 1  $\mu$ M BQ-788 (a selective ET<sub>B</sub> receptor antagonist), 200 ng·mL<sup>-1</sup> PTX (a selective G<sub>i</sub> protein inhibitor) and 100  $\mu$ M NF449 (a G<sub>s</sub> protein inhibitor) had no effect on the ET-1-induced inhibition of insulin-stimulated Akt phosphorylation.

### Involvement of GRK2 in the ET-1-induced inhibition of insulin-stimulated Akt phosphorylation in L6 myotubes

As shown in Figure 5, overexpression of GFP as a control or GRK2-ct, a dominant negative construct lacking the N-terminal kinase domain (Koch *et al.*, 1994; Kurose *et al.*, 1999), had no effect on the insulin-stimulated Akt phosphorylation at Thr<sup>308</sup> and Ser<sup>473</sup>. In L6 myotubes overexpressing GFP, treatment with ET-1 for 2 and 5 min decreased the phosphorylation levels of Akt at Thr<sup>308</sup> and Ser<sup>473</sup> induced by treatment with 100 nM insulin for 60 min (Figure 5). The inhibition by ET-1 of insulin-stimulated Akt phosphorylation was abolished in cells overexpressing GRK2-ct.

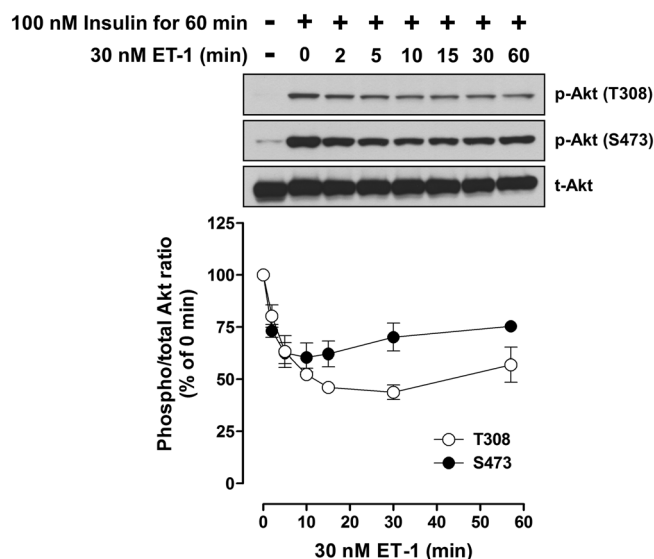


**Figure 3**

Effect of ET-1 on Akt phosphorylation in response to 60 min exposure to 100 nM insulin in L6 myotubes. The cells were treated with 30 nM ET-1 for indicated times during treatment with 100 nM insulin for 60 min. Representative immunoblots were obtained using antibodies to phospho-Akt at Thr<sup>308</sup> [p-Akt (T308)], phospho-Akt at Ser<sup>473</sup> [p-Akt (S473)] and total Akt (t-Akt). Ordinate represents Akt phosphorylation responses, which are normalized to the level of insulin-stimulated Akt phosphorylation in L6 myotubes without treatment with ET-1. Data are presented as means  $\pm$  SEM of the results obtained from five to six experiments. When no error bar is shown, the error is smaller than the symbol.

In L6 myotubes transfected with non-targeting siRNA (control siRNA), ET-1 inhibited the insulin-stimulated Akt phosphorylation at Thr<sup>308</sup> and Ser<sup>473</sup> (Figure 6). However, GRK2 knockdown by GRK2 siRNA prevented the ET-1-induced inhibition of insulin-stimulated Akt phosphorylation.

### Effects of insulin on [<sup>3</sup>H]2-DG uptake in L6 myotubes

Insulin increased the rate of [<sup>3</sup>H]2-DG uptake in myotubes (Figure 7B), whereas it failed to facilitate [<sup>3</sup>H]2-DG uptake in L6 myoblasts (data not shown), indicating that the insulin-stimulated glucose uptake is a myotube-specific response. In the absence of insulin, there was a low basal uptake rate of [<sup>3</sup>H]2-DG (Figure 7B). Treatment of L6 myotubes with 100 nM insulin for 2 h increased [<sup>3</sup>H]2-DG uptake and the insulin-stimulated [<sup>3</sup>H]2-DG uptake was inhibited by the PI3K inhibitors, GSK2126458 or LY294002, both of which did not affect the basal [<sup>3</sup>H]2-DG uptake rate (Figure 7B). Insulin (3–300 nM) increased [<sup>3</sup>H]2-DG uptake rate in a concentration-dependent manner with a pEC<sub>50</sub> value of  $8.08 \pm 0.11$ . The maximal response induced by 100 nM insulin was  $155 \pm 5\%$  of the basal uptake rate ( $n = 12$ ) (Figure 7C). ET-1 (30 nM) non-competitively antagonized insulin-stimulated [<sup>3</sup>H]2-DG uptake, without affecting the pEC<sub>50</sub> value (pEC<sub>50</sub>:  $7.86 \pm 0.29$ ,  $n = 6$ ) calculated from each concentration-response curve.

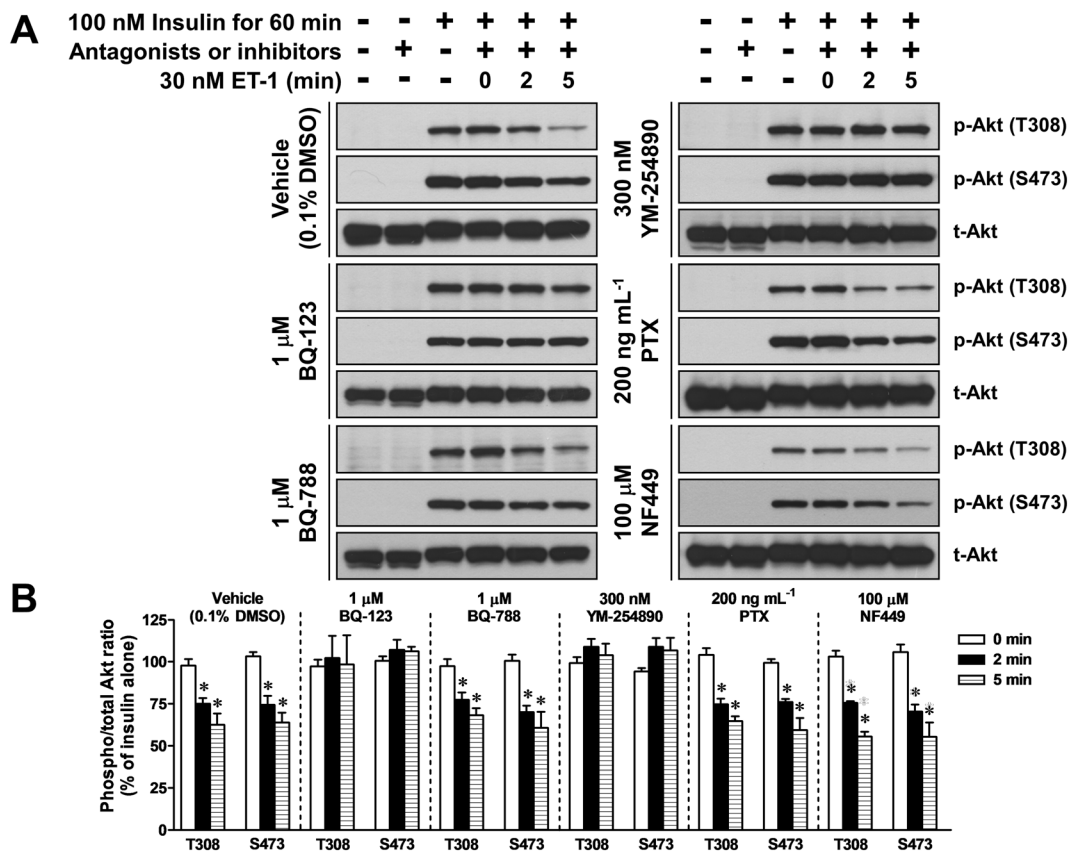


**Figure 4**

Effects of 0.1% DMSO (as a vehicle), BQ-123 (a selective  $ET_A$  receptor antagonist), BQ-788 (a selective  $ET_B$  receptor antagonist), YM-254890 (a selective  $G_q$  protein inhibitor), PTX (a selective  $G_i$  protein inhibitor) and NF449 (a  $G_s$  protein inhibitor) on the ET-1-induced inhibition of insulin-stimulated Akt phosphorylation in L6 myotubes. The cells were treated with 30 nM ET-1 for indicated times during treatment with 100 nM insulin for 60 min. The cells were treated with one of the drugs for 30 min (except PTX for 18 h) before treatment with 100 nM insulin for 60 min. (A) Representative immunoblots obtained using antibodies to phospho-Akt at Thr<sup>308</sup> [p-Akt (T308)], phospho-Akt at Ser<sup>473</sup> [p-Akt (S473)] and total Akt (t-Akt). (B) ET-1-induced changes in the ratio of phosphorylated Akt to t-Akt. Ordinate represents Akt phosphorylation responses, which are normalized to the level of insulin-stimulated Akt phosphorylation in L6 myotubes without treatment with ET-1, vehicle, antagonists or inhibitors. Data are presented as means  $\pm$  SEM of the results obtained from five to six experiments. \* $P < 0.05$  versus its control (100 nM insulin alone).

### Molecular mechanisms for ET-1-induced inhibition of insulin-stimulated [<sup>3</sup>H]2-DG uptake in L6 myotubes

In L6 myotubes, treatment with ET-1 or BQ-123, overexpression of GRK2-ct and transfection of GRK2 siRNA had no effect on the basal [<sup>3</sup>H]2-DG uptake rate in the absence of insulin stimulation (data not shown). ET-1 (30 nM) inhibited the insulin-stimulated [<sup>3</sup>H]2-DG uptake (Figure 8A). The inhibitory effect of ET-1 was cancelled by pretreatment with 1  $\mu$ M BQ-123 (Figure 8A). Notably, the ET-1-induced inhibition of insulin-stimulated [<sup>3</sup>H]2-DG uptake was also blocked by either overexpression of GRK2-ct ( $n = 8$ ) (Figure 8B) or GRK2 knockdown ( $n = 6$ ) (Figure 8C).

### Augmentation by ET-1 stimulation of interaction of Akt with GRK2 in L6 myotubes

Co-immunoprecipitation assays showed that endogenous Akt was nonspecifically immunoprecipitated with mouse normal IgG (control IgG) under resting condition (Figure 9A). Treatment of myotubes with 30 nM ET-1 for 5 or 10 min resulted in

approximately 2.5-fold increase in the amount of Akt protein co-immunoprecipitated with FLAG-GRK2, compared with the basal interaction, without ET-1 stimulation (Figure 9B). Unexpectedly, insulin stimulation alone augmented the interaction of Akt with FLAG-GRK2 in the absence of ET-1 stimulation, and the augmentation by insulin of the interaction was markedly attenuated by ET-1 stimulation for 10 min (Figure 9C). Accordingly, there was a discrepancy in the effect of ET-1 on the insulin-stimulated Akt phosphorylation between FLAG-GRK2-negative and positive cells, that is, ET-1 inhibited the insulin-stimulated Akt phosphorylation in L6 myotubes not overexpressing FLAG-GRK2 (Figure-3), whereas the inhibitory effect of ET-1 was not observed in the cells overexpressing FLAG-GRK2 (data not shown).

## Discussion

In the present study, we have investigated the mechanism(s) underlying ET-1-induced insulin resistance using L6 myotubes. We demonstrated that ET-1 inhibited insulin-stimulated Akt

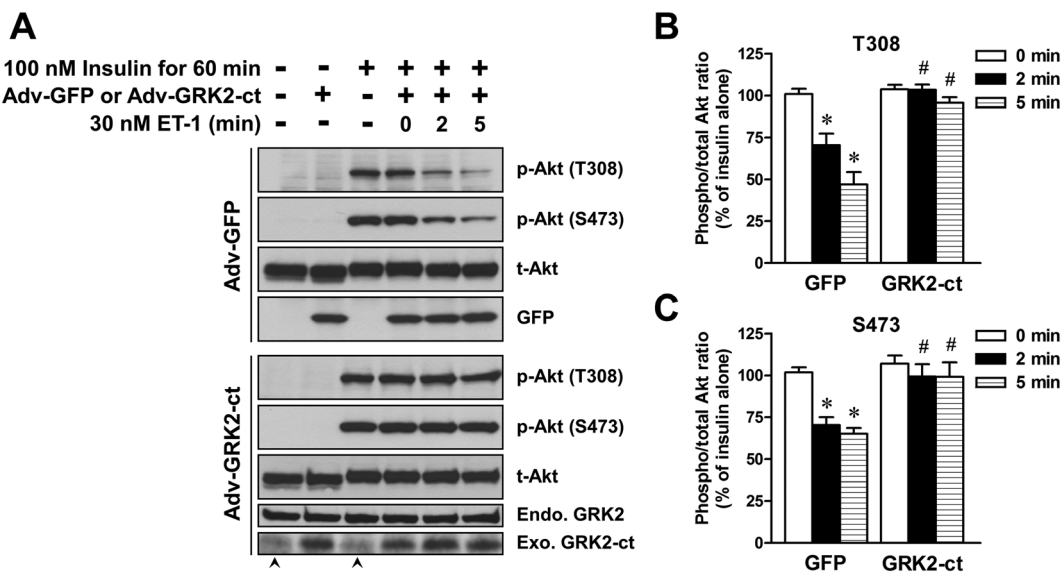


**Figure 5**

Effects of introducing GFP (Adv-GFP) and GRK2-ct (Adv-GRK2-ct) by adenovirus infection on the ET-1-induced inhibition of insulin-stimulated Akt phosphorylation in L6 myotubes. The cells were treated with 30 nM ET-1 for indicated times during treatment with 100 nM insulin for 60 min. (A) Representative immunoblots obtained using antibodies to phospho-Akt at Thr<sup>308</sup> [p-Akt (T308)], phospho-Akt at Ser<sup>473</sup> [p-Akt (S473)], total Akt (t-Akt), GFP and GRK2. Endogenously expressing GRK2 (Endo. GRK2) and exogenously expressing GRK2-ct (Exo. GRK2-ct) were detected with GRK2 antibody (C-15), which binds to the GRK2-ct. Arrow head indicates a non-specific band in the lane of Exo. GRK2-ct. (B and C) ET-1-induced changes in the ratio of phosphorylated Akt to t-Akt. Ordinate represents Akt phosphorylation responses, which are normalized to the level of insulin-stimulated Akt phosphorylation in L6 myotubes without treatment with ET-1 and adenovirus. Data are presented as means ± SEM of the results obtained from six experiments. \**P* < 0.05 versus its control (100 nM insulin alone). #*P* < 0.05 versus Adv-GFP-treated cells.

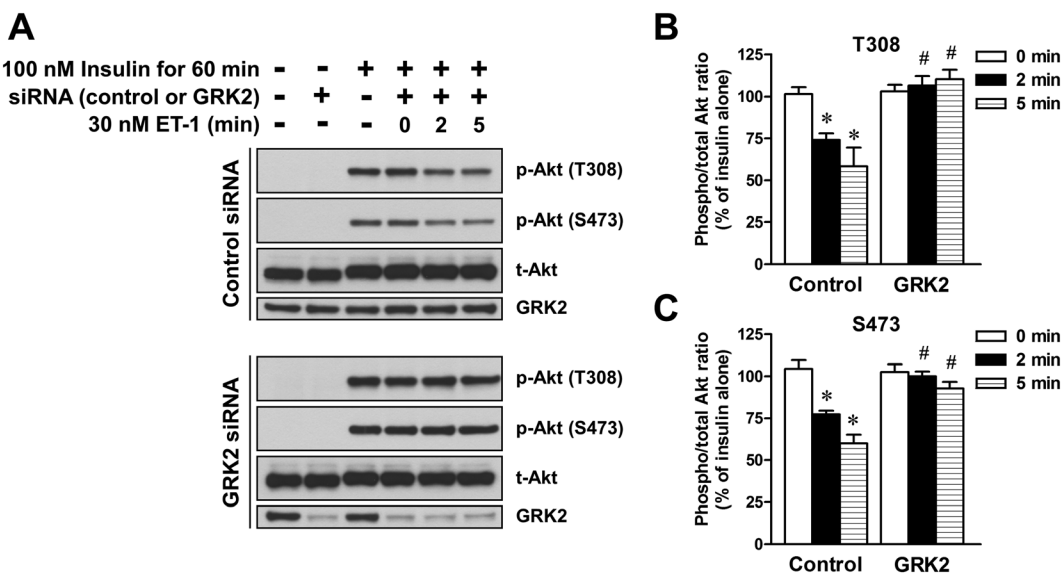


**Figure 6**

Effects of introducing control and GRK2 siRNA on the ET-1-induced inhibition of insulin-stimulated Akt phosphorylation in L6 myotubes. The cells were treated with 30 nM ET-1 for indicated times during treatment with 100 nM insulin for 60 min. (A) Representative immunoblots obtained using antibodies to phospho-Akt at Thr<sup>308</sup> [p-Akt (T308)], phospho-Akt at Ser<sup>473</sup> [p-Akt (S473)], total Akt (t-Akt) and GRK2. (B and C) ET-1 induced changes in the ratio of phosphorylated Akt to t-Akt. Ordinate represents Akt phosphorylation responses, which are normalized to the level of insulin-stimulated Akt phosphorylation in L6 myotubes without treatment with ET-1 and siRNA. Data are presented as means ± SEM of the results obtained from six experiments. \**P* < 0.05 versus its control (100 nM insulin alone). #*P* < 0.05 versus control siRNA-treated cells.

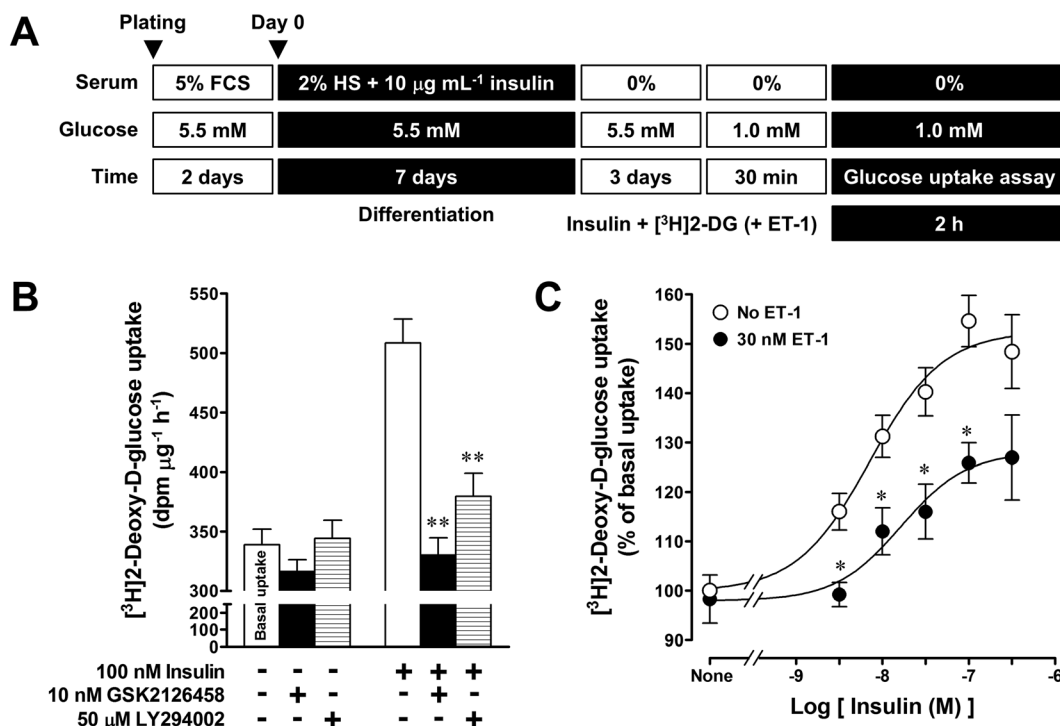


Figure 7

Characterization of insulin-stimulated [ $^3\text{H}$ ]2-DG uptake in L6 myotubes. (A) Protocol for [ $^3\text{H}$ ]2-DG uptake assay. (B) Effects of GSK2126458 and LY294002 on insulin-stimulated [ $^3\text{H}$ ]2-DG uptake. The cells were treated with the inhibitor for 30 min before stimulation with insulin. Ordinate represents the rate of [ $^3\text{H}$ ]2-DG uptake ( $\text{dpm}\cdot\mu\text{g}^{-1}\cdot\text{h}^{-1}$ ). (C) concentration-response curves for insulin-stimulated [ $^3\text{H}$ ]2-DG uptake in the absence and presence of 30 nM ET-1. Ordinate represents percentage of the rate of [ $^3\text{H}$ ]2-DG uptake, which is normalized to basal [ $^3\text{H}$ ]2-DG uptake before application of insulin and ET-1. Data are presented as means  $\pm$  SEM of the results obtained from eight experiments. \* $P < 0.05$ , \*\* $P < 0.01$  versus its control (insulin alone).

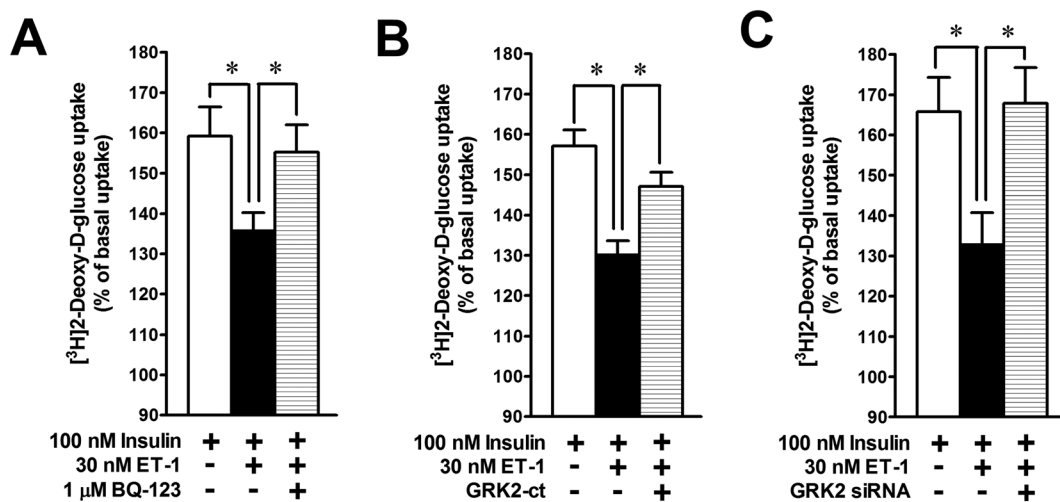
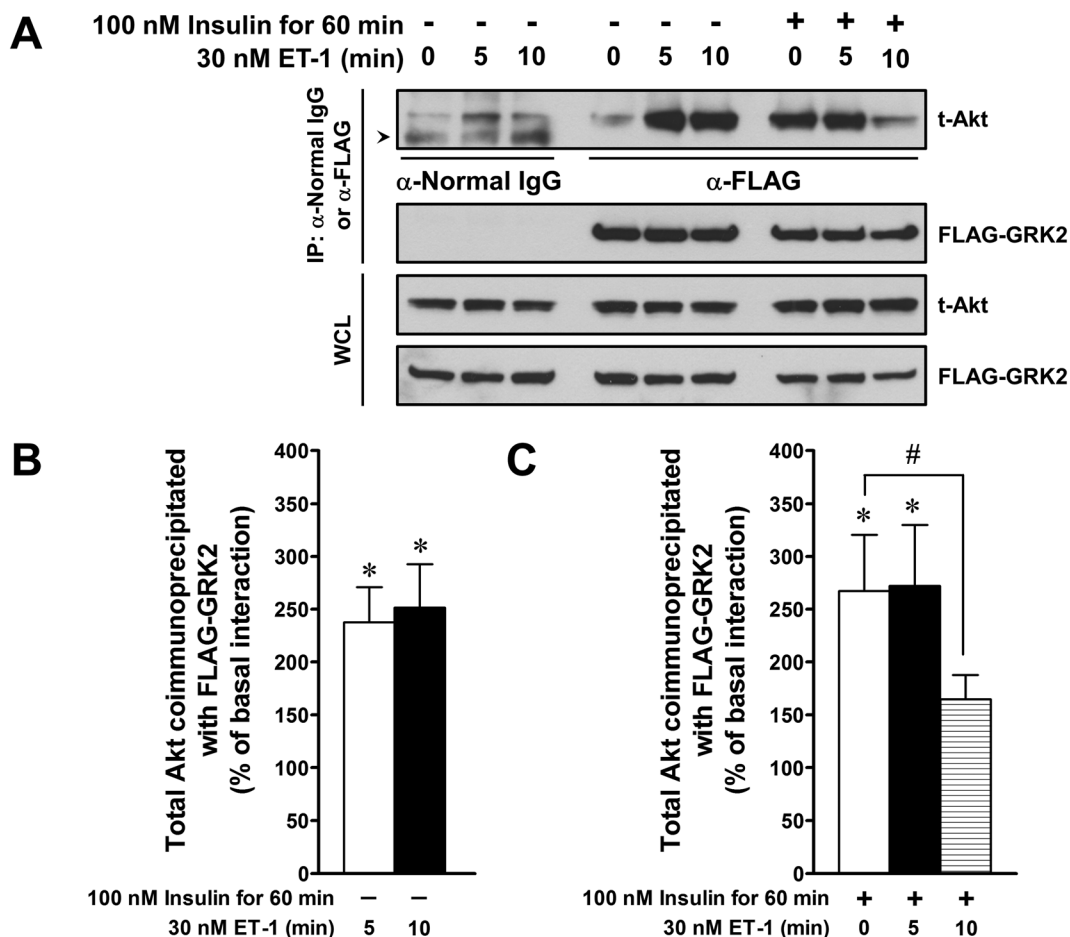


Figure 8

Effects of BQ-123 (A), GRK2-ct overexpression (B) and GRK2 knockdown (C) on the ET-1-induced inhibition of insulin-stimulated [ $^3\text{H}$ ]2-DG uptake in L6 myotubes. ET-1 was given concomitantly with insulin and [ $^3\text{H}$ ]2-DG. Ordinate represents percentage of the rate of [ $^3\text{H}$ ]2-DG uptake, which is normalized to basal [ $^3\text{H}$ ]2-DG uptake before application of insulin and ET-1. Data are presented as means  $\pm$  SEM of the results obtained from six to eight experiments. \* $P < 0.05$  between indicated columns.



**Figure 9**

Interaction of endogenous Akt with FLAG-GRK2 in L6 myotubes. (A) Upper panel for immunoprecipitated samples (IP:  $\alpha$ -normal IgG or FLAG): FLAG-tagged GRK2 proteins were immunoprecipitated with anti-FLAG antibody. Immunoprecipitates were probed with the anti-total Akt (t-Akt) antibody to estimate co-immunoprecipitated endogenous Akt. Arrow head indicates a non-specific band (lower band) for  $\alpha$ -normal IgG in the lane of t-Akt. Lower panel for IP: FLAG-tagged GRK2 proteins were immunoprecipitated with anti-FLAG antibody, and the immunoprecipitates were probed with the anti-FLAG-HRP antibody to normalize the quantity of co-immunoprecipitated endogenous Akt. Upper panel for whole cell lysate (WCL): the expressed Akt was detected with the anti-t-Akt antibody. Lower panel for WCL: the expressed FLAG-GRK2 was detected with the anti-FLAG-HRP antibody. (B and C) The histogram represents change in the ratio of the quantity of immunoprecipitated endogenous Akt to that of immunoprecipitated FLAG-GRK2. The change is normalized to the interaction of Akt with FLAG-GRK2 under resting conditions before application of insulin and ET-1. Data are presented as means  $\pm$  SEM of the results obtained from six experiments. \* $P < 0.05$  versus basal interaction (in the absence of insulin and ET-1). # $P < 0.05$  between indicated columns.

phosphorylation and glucose uptake in L6 myotubes and that the ET<sub>A</sub> receptor-G<sub>q</sub> protein pathway and GRK2 were involved in the inhibitory effects of ET-1 (Figure 10).

The L6 skeletal muscle cell line is widely used as a model for studying glucose transport and myogenesis. L6 myoblasts have the potential ability to spontaneously differentiate into myotubes (Nevzorova *et al.*, 2002). To differentiate L6 myoblasts into myotubes, we used differentiation medium containing both 2% HS and 10  $\mu\text{g}\cdot\text{mL}^{-1}$  insulin, although many investigators have used the medium supplemented with either one of 2% FCS (Nevzorova *et al.*, 2002), 2% HS (Ruest *et al.*, 2002) or 10  $\mu\text{g}\cdot\text{mL}^{-1}$  insulin (Jin *et al.*, 1991). The criteria for differentiation of myoblasts into myotubes are as follows: (i) multinucleation, (ii) spontaneous contraction, (iii) an increase in expression level of transcription factors such as MyoD and myogenin and (iv)

an increase in expression level of GLUT4 (Bentzinger *et al.*, 2012; Mitsumoto *et al.*, 1991; Mitsumoto and Klip, 1992; Öberg *et al.*, 2011). The L6 myotubes differentiated in differentiation medium containing both 2% HS and 10  $\mu\text{g}\cdot\text{mL}^{-1}$  insulin fulfil the earlier criteria, indicating that these myotubes consist of highly differentiated (mature) skeletal muscle cells.

In the differentiated L6 myotubes, insulin stimulated PI3K-dependent Akt phosphorylation (Figure 2C and D) and [<sup>3</sup>H]2-DG uptake (an index of glucose uptake; Figure 7B). These results are consistent with previous studies showing that the PI3K inhibitors, wortmannin and LY 294002, inhibited insulin-stimulated Akt phosphorylation and glucose uptake in skeletal muscle cells (Nevzorova *et al.*, 2002; Shepherd *et al.*, 1997; Tsakiridis *et al.*, 1995) and indicate that L6 myotubes used in the present study possess functional

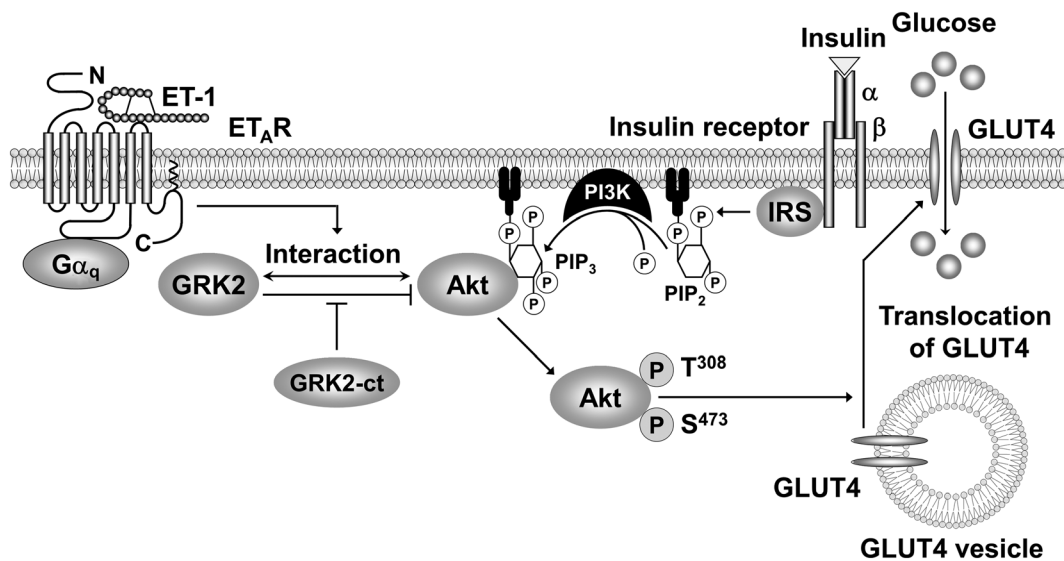


**Figure 10**

A schematic diagram showing the pathways leading to the negative regulation of insulin signalling by ET-1 in L6 myotubes.

InsR and InsR-stimulated intracellular signalling pathway leading to GLUT4. Indeed, expression of InsR, IRS-1, Akt and GLUT4 in L6 myotubes was demonstrable by RT-PCR (Supporting Information Fig. S1) or Western blot analysis (Supporting Information Fig. S3).

Several studies have demonstrated that in adipocytes, insulin stimulates GLUT4-mediated glucose uptake through an IRS-independent pathway in addition to the classical IRS-dependent pathway (Imamura *et al.*, 1999; Usui *et al.*, 2005; Usui *et al.*, 2003). In adipocytes, insulin stimulation can activate a  $G_{\alpha_q}$  protein independently of IRS, and the activated  $G_{\alpha_q}$  subunit stimulates GLUT4-mediated glucose uptake through activation of Cdc42 and PI3K (Imamura *et al.*, 1999; Usui *et al.*, 2005; Usui *et al.*, 2003). This raises the possibility that activation of  $G_q$  protein is involved in the insulin-stimulated PI3K-dependent Akt phosphorylation in L6 myotubes. However, this possibility was ruled out on the basis of insensitivity to YM-254890, a selective  $G_q$  protein inhibitor (Supporting Information Fig. S4).

The present study has shown that in L6 myotubes, ET-1 inhibits insulin-stimulated Akt phosphorylation (Figure 3) and [ $^3$ H]2-DG uptake (Figure 7), as reported previously (Shemyakin *et al.*, 2011). In our recent report, we have shown that in L6 myoblasts, both  $ET_A$  and  $ET_B$  receptors are expressed at mRNA level (Harada *et al.*, 2014). The  $ET_A$  receptors can couple with  $G_q$  and  $G_s$  proteins, while  $ET_B$  receptors couple to  $G_q$  and  $G_i$  proteins (Alexander *et al.*, 2011). Based on the sensitivity to several types of antagonists and inhibitors (Figure 4), the ET-1-induced inhibition of the insulin-stimulated Akt phosphorylation and [ $^3$ H]2-DG uptake is considered to be mediated through the  $ET_A$  receptor- $G_q$  protein pathway. The dominant role of this pathway in L6 myotubes is consistent with that in the ET-1-induced ERK1/2 phosphorylation and  $Ca^{2+}$  influx in L6 myoblasts, as shown in our recent report (Harada *et al.*, 2014). These findings support clinical evidence that selective

blockade of  $ET_A$  receptors improves insulin-mediated glucose uptake in obese subjects (Lteif *et al.*, 2007).

The present study has demonstrated that the ET-1-mediated inhibition of insulin's action results from the augmented interaction of GRK2 with Akt and the subsequent inhibition of insulin-stimulated Akt phosphorylation. This conclusion is based on (i) attenuation of the ET-1-mediated inhibition of insulin-stimulated Akt phosphorylation and glucose uptake following overexpression of GRK2-ct (Figures 5, 8) or GRK2 knockdown by siRNA (Figures 6, 8) and (ii) augmentation by ET-1 of association between Akt and GRK2. GRK2 consists of an N-terminus kinase domain and a C-terminus containing the pleckstrin homology domain, which is involved in the binding of GRK2 to several signalling molecules such as  $G_{\beta\gamma}$  subunits and Akt (Evron *et al.*, 2012; Liu *et al.*, 2005). Because GRK2-ct lacks the N-terminus kinase domain, but it retains the ability to bind to other molecules, it can function as a dominant-negative form of GRK2 (Koch *et al.*, 1994; Nishida *et al.*, 2000), which interferes with the interaction between GRK2 and its binding partner molecules. In fact, GRK2 is reported to interact with Akt via its C-terminal region in rat endothelial cells (functionally disturbed by a pathological process such as diabetes mellitus) to reduce Akt phosphorylation (Liu *et al.*, 2005). Taken together, the present findings strongly indicate that GRK2 inhibits insulin-stimulated Akt phosphorylation, by interacting with Akt via its C-terminal region.

Unexpectedly, in L6 myotubes overexpressing FLAG-GRK2, insulin augmented the binding of Akt to FLAG-GRK2, and the augmentation was inhibited by ET-1 treatment for 10 min. The inhibitory effect of ET-1 on the insulin-stimulated interaction of overexpressed FLAG-GRK2 with Akt might be due to the  $\beta\gamma$  subunits released from  $G_{\alpha_q}$  protein upon activation of  $ET_A$  receptors competing with Akt for the C-terminus region of FLAG-GRK2. The

insulin-stimulated interaction of FLAG-GRK2 with Akt might inhibit phosphorylation of Akt like the ET-1-stimulated interaction, resulting in loss of ET-1-induced, GRK2-mediated inhibition of insulin-stimulated Akt phosphorylation. Further studies will be required to clarify the mechanism for insulin-stimulated interaction of FLAG-GRK2 with Akt.

In addition to Akt, IRS-1 is a potential target for ET-1-induced, GRK2-mediated inhibition of insulin-stimulated glucose uptake (Usui *et al.*, 2005; Usui *et al.*, 2004). IRS-1 is one of the major substrates of the InsR kinase, and it contains multiple Ser/Thr phosphorylation sites (Leto and Saltiel, 2012). There are two possible mechanisms involved here. One is that the ET-1-induced inhibition of insulin signalling results from the interaction of IRS-1 with GRK2 and the other, that GRK2 mediated phosphorylation of IRS-1. In the present study, the interaction of IRS-1 with GRK2 was not detected by a co-immunoprecipitation assay in L6 myotubes overexpressing FLAG-GRK2 (Supporting Information Fig. S3). The possible involvement of GRK2-mediated IRS-1 phosphorylation in the ET-1-induced, GRK2-dependent insulin resistance will be studied in the future.

## Conclusions

In summary, the present study has shown the mechanism for the ET-1-induced inhibition of insulin signalling (i.e. insulin resistance) in L6 myotubes, as summarized in Figure 10. In L6 myotubes, insulin stimulates the PI3K-dependent Akt phosphorylation, which facilitates glucose uptake by augmenting translocation of GLUT4 to the plasma membrane. Activation of ET<sub>A</sub> receptors with ET-1 facilitates the interaction of GRK2 with Akt via a G<sub>q</sub> protein-dependent pathway. Overexpression of GRK2-ct counteracts ET-1-induced, GRK2-mediated inhibition of the insulin-stimulated Akt phosphorylation and glucose uptake. Thus, activation of ET<sub>A</sub> receptors with ET-1 induces the insulin resistance by facilitating the interaction of GRK2 with Akt. These results indicate that both ET<sub>A</sub> receptors and GRK2 are therapeutic targets for overcoming insulin resistance

## Acknowledgements

We thank Dr. Hitoshi Kurose (Kyusyu University, Japan) for kindly donating recombinant adenoviruses encoding GFP and GRK2-ct, and the pcDNA3 mammalian expression vector encoding FLAG-GRK2. We also thank Astellas Pharma Inc. (Tokyo, Japan) for generously providing YM-254890. This study was supported in part by Grants-in-Aid for Scientific Research (C) from Japan Society for the Promotion of Science (grant 24590309) (to T. H.), Grants-in-Aid for Scientific Research (B) from Japan Society for the Promotion of Science (grant 24390059) (to S. M.) and by grants from Smoking Research Foundation of Japan (to S. M.), the Pharmacological Research Foundation, Tokyo (to T. H.), Suzuken Memorial Foundation (to T. H.) and Actelion Pharmaceuticals Japan Ltd. (to T. H.).

## Author contributions

T. H., A. H., T. H., T. H., S. K., K. T., T. H., Y. M., P. N. and Y. M. performed the research. T. H., A. H. and S. M. designed the research study. T. H., T. H. and S. M. provided funding. T. H. and S. M. wrote the manuscript.

## Conflict of interest

The authors state no conflict of interest.

## References

- Alexander SPH, Davenport AP, Kelly E, Marrion N, Peters JA, Benson HE, *et al.* (2015a). The Concise Guide to PHARMACOLOGY 2015/16: G Protein-Coupled Receptors. *Br J Pharmacol* 172: 5744–5869.
- Alexander SPH, Fabbro D, Kelly E, Marrion N, Peters JA, Benson HE, *et al.* (2015b). The Concise Guide to PHARMACOLOGY 2015/16: Catalytic receptors. *Br J Pharmacol* 172: 5979–6023.
- Alexander SPH, Fabbro D, Kelly E, Marrion N, Peters JA, Benson HE, *et al.* (2015c). The Concise Guide to PHARMACOLOGY 2015/16: Enzymes. *Br J Pharmacol* 172: 6024–6109.
- Alexander SPH, Kelly E, Marrion N, Peters JA, Benson HE, Faccenda E, *et al.* (2015d). The Concise Guide to PHARMACOLOGY 2015/16: Transporters. *Br J Pharmacol* 172: 6110–6202.
- Alexander SP, Mathie A, Peters JA (2011). *Guide to Receptors and Channels (GRAC)*, 5th edition. *Br J Pharmacol* 164: S1–S324.
- Bentzinger CF, Wang YX, Rudnicki MA (2012). Building muscle: molecular regulation of myogenesis. *Cold Spring Harb Perspect Biol* 4: ID a008342.
- Bradford MM (1976). A rapid and sensitive method for the quantitation of microgram quantities of protein utilizing the principle of protein–dye binding. *Anal Biochem* 72: 248–254.
- Curtis MJ, Bond RA, Spina D, Ahluwalia A, Alexander SPH, Giembycz MA, *et al.* (2015). Experimental design and analysis and their reporting: new guidance for publication in *BJP*. *Br J Pharmacol* 172: 3461–3471.
- DeFronzo RA (1988). Lilly lecture 1987. The triumvirate: beta-cell, muscle, liver. A collusion responsible for NIDDM. *Diabetes* 37: 667–687.
- Evron T, Daigle TL, Caron MG (2012). GRK2: multiple roles beyond G protein-coupled receptor desensitization. *Trends Pharmacol Sci* 33: 154–164.
- Ferri C, Bellini C, Desideri G, Di Francesco L, Baldoncini R, Santucci A, *et al.* (1995). Plasma endothelin-1 levels in obese hypertensive and normotensive men. *Diabetes* 44: 431–436.
- Gomes AR, Soares AG, Peviani S, Nascimento RB, Moriscot AS, Salvini TF (2006). The effect of 30 minutes of passive stretch of the rat soleus muscle on the myogenic differentiation, myostatin, and atrogen-1 gene expressions. *Arch Phys Med Rehabil* 87: 241–246.
- Harada T, Horinouchi T, Higa T, Hoshi A, Higashi T, Terada K, *et al.* (2014). Endothelin-1 activates extracellular signal-regulated kinases 1/2 via transactivation of platelet-derived growth factor receptor in rat L6 myoblasts. *Life Sci* 104: 24–31.

- Horinouchi T, Higashi T, Higa T, Terada K, Mai Y, Aoyagi H, *et al.* (2012). Different binding property of STIM1 and its novel splice variant STIM1L to Orai1, TRPC3, and TRPC6 channels. *Biochem Biophys Res Commun* 428: 252–258.
- Horinouchi T, Terada K, Higashi T, Miwa S (2013). Endothelin receptor signaling: new insight into its regulatory mechanisms. *J Pharmacol Sci* 123: 85–101.
- Imamura T, Völlenweider P, Egawa K, Clodi M, Ishibashi K, Nakashima N, *et al.* (1999). G alpha-q/11 protein plays a key role in insulin-induced glucose transport in 3 T3-L1 adipocytes. *Mol Cell Biol* 19: 6765–6774.
- Jin P, Sejersen T, Ringertz NR (1991). Recombinant platelet-derived growth factor-BB stimulates growth and inhibits differentiation of rat L6 myoblasts. *J Biol Chem* 266: 1245–1249.
- Kamikawa Y, Ikeda S, Harada K, Ohwatashi A, Yoshida A (2013). Passive repetitive stretching for a short duration within a week increases myogenic regulatory factors and myosin heavy chain mRNA in rats' skeletal muscles. *Scientific World Journal* 2013: ID 493656.
- Kim I, Yang D, Tang X, Carroll JL (2011). Reference gene validation for qPCR in rat carotid body during postnatal development. *BMC Res Notes* 4: ID 440.
- Knight SD, Adams ND, Burgess JL, Chaudhari AM, Darcy MG, Donatelli CA, *et al.* (2010). Discovery of GSK2126458, a highly potent inhibitor of PI3K and the mammalian target of rapamycin. *ACS Med Chem Lett* 1: 39–43.
- Koch WJ, Hawes BE, Inglese J, Luttrell LM, Lefkowitz RJ (1994). Cellular expression of the carboxyl terminus of a G protein-coupled receptor kinase attenuates G<sub>βγ</sub>-mediated signaling. *J Biol Chem* 269: 6193–6197.
- Kurose H, Nishida M, Nagao T (1999). β<sub>γ</sub> subunit of heterotrimeric G protein as a new target molecule for drug development. *Folia Pharmacol Jpn* 114: 75–80.
- Laplante M, Sabatini DM (2012). mTOR signaling in growth control and disease. *Cell* 149: 274–293.
- Lerman A, Edwards BS, Hallett JW, Heublein DM, Sandberg SM, Burnett JCJ (1991). Circulating and tissue endothelin immunoreactivity in advanced atherosclerosis. *N Engl J Med* 325: 997–1001.
- Leto D, Saltiel AR (2012). Regulation of glucose transport by insulin: traffic control of GLUT4. *Nat Rev Mol Cell Biol* 13: 383–396.
- Liu S, Premont RT, Kontos CD, Zhu S, Rockey DC (2005). A crucial role for GRK2 in regulation of endothelial cell nitric oxide synthase function in portal hypertension. *Nat Med* 11: 952–958.
- Lteif A, Vaishnava P, Baron AD, Mather KJ (2007). Endothelin limits insulin action in obese/insulin-resistant humans. *Diabetes* 56: 728–734.
- Mitsumoto Y, Burdett E, Grant A, Klip A (1991). Differential expression of the GLUT1 and GLUT4 glucose transporters during differentiation of L6 muscle cells. *Biochem Biophys Res Commun* 175: 652–659.
- Mitsumoto Y, Klip A (1992). Development regulation of the subcellular distribution and glycosylation of GLUT1 and GLUT4 glucose transporters during myogenesis of L6 muscle cells. *J Biol Chem* 267: 4957–4962.
- Nevzorova J, Bengtsson T, Evans BA, Summers RJ (2002). Characterization of the β-adrenoceptor subtype involved in mediation of glucose transport in L6 cells. *Br J Pharmacol* 137: 9–18.
- Nishida M, Maruyama Y, Tanaka R, Kontani K, Nagao T, Kurose H (2000). G α<sub>i</sub> and G α<sub>o</sub> are target proteins of reactive oxygen species. *Nature* 408: 492–495.
- Öberg A, Dehvari N, Bengtsson T (2011). β-Adrenergic inhibition of contractility in L6 skeletal muscle cells. *PLoS One* 6: e22304.
- Obici S, Feng Z, Karkanas G, Baskin DG, Rossetti L (2002). Decreasing hypothalamic insulin receptors causes hyperphagia and insulin resistance in rats. *Nat Neurosci* 5: 566–572.
- Ottosson-Seeberger A, Lundberg JM, Alvestrand A, Ahlborg G (1997). Exogenous endothelin-1 causes peripheral insulin resistance in healthy humans. *Acta Physiol Scand* 161: 211–220.
- Pawson AJ, Sharman JL, Benson HE, Faccenda E, Alexander SPH, Buneman OP *et al.*, NC-IUPHAR (2014) The IUPHAR/BPS Guide to PHARMACOLOGY: an expert-driven knowledge base of drug targets and their ligands. *Nucl. Acids Res.* 42 (Database Issue): D1098–1106.
- Pernow J, Shemyakin A, Böhm F (2012). New perspectives on endothelin-1 in atherosclerosis and diabetes mellitus. *Life Sci* 91: 507–516.
- Rodríguez-Pascual F, Busnadiego O, Lagares D, Lamas S (2011). Role of endothelin in the cardiovascular system. *Pharmacol Res* 63: 463–472.
- Rubin LJ (2012). Endothelin receptor antagonists for the treatment of pulmonary artery hypertension. *Life Sci* 91: 517–521.
- Ruest LB, Marcotte R, Wang E (2002). Peptide elongation factor eEF1A-2/S1 expression in cultured differentiated myotubes and its protective effect against caspase-3-mediated apoptosis. *J Biol Chem* 277: 5418–5425.
- Sarbassov DD, Guertin DA, Ali SM, Sabatini DM (2005). Phosphorylation and regulation of Akt/PKB by the rictor-mTOR complex. *Science* 307: 1098–1101.
- Schalin-Jääntti C, Yki-Järvinen H, Koranyi L, Bourey R, Lindström J, Nikula-Ijäs P, *et al.* (1994). Effect of insulin on GLUT4 mRNA and protein concentrations in skeletal muscle of patients with NIDDM and their first-degree relatives. *Diabetologia* 37: 401–407.
- Shemyakin A, Salehzadeh F, Esteves Duque-Guimaraes D, Böhm F, Rullman E, Gustafsson T, *et al.* (2011). Endothelin-1 reduces glucose uptake in human skeletal muscle in vivo and in vitro. *Diabetes* 60: 2061–2067.
- Shepherd PR, Nave BT, Rincon J, Haigh RJ, Foulstone E, Proud C, *et al.* (1997). Involvement of phosphoinositide 3-kinase in insulin stimulation of MAP-kinase and phosphorylation of protein kinase-B in human skeletal muscle: implications for glucose metabolism. *Diabetologia* 40: 1172–1177.
- Shisheva A (2008). Phosphoinositides in insulin action on GLUT4 dynamics: not just PtdIns(3,4,5)P<sub>3</sub>. *Am J Physiol Endocrinol Metab* 293: E536–E544.
- Takahashi K, Ghatei MA, Lam HC, O'Halloran DJ, Bloom SR (1990). Elevated plasma endothelin in patients with diabetes mellitus. *Diabetologia* 33: 306–310.
- Touyz RM, Schiffrin EL (2003). Role of endothelin in human hypertension. *Can J Physiol Pharmacol* 81: 533–541.
- Tsakiridis T, McDowell HE, Walker T, Downes CP, Hundal HS, Vranic M, *et al.* (1995). Multiple roles of phosphatidylinositol 3-kinase in regulation of glucose transport, amino acid transport, and glucose transporters in L6 skeletal muscle cells. *Endocrinology* 136: 4315–4322.
- Usui I, Imamura T, Babendure JL, Satoh H, Lu JC, Hupfeld CJ, *et al.* (2005). G protein-coupled receptor kinase 2 mediates endothelin-1-induced insulin resistance via the inhibition of both Gαq/11 and insulin receptor substrate-1 pathways in 3 T3-L1 adipocytes. *Mol Endocrinol* 19: 2760–2768.
- Usui I, Imamura T, Huang J, Satoh H, Olefsky JM (2003). Cdc42 is a Rho GTPase family member that can mediate insulin signaling to glucose transport in 3 T3-L1 adipocytes. *J Biol Chem* 278: 13765–13774.

Usui I, Imamura T, Satoh H, Huang J, Babendure JL, Hupfeld CJ, *et al.* (2004). GRK2 is an endogenous protein inhibitor of the insulin signaling pathway for glucose transport stimulation. *EMBO J* 23: 2821–2829.

Yanagisawa M, Kurihara H, Kimura S, Tomobe Y, Kobayashi M, Mitsui Y, *et al.* (1988). A novel potent vasoconstrictor peptide produced by vascular endothelial cells. *Nature* 332: 411–415.

## Supporting Information

Additional Supporting Information may be found in the on-line version of this article at the publisher's web-site:

<http://dx.doi.org/10.1111/bph.13406>

**Figure S1** Changes in mRNA expression level for ET<sub>A</sub> receptors (A), G<sub>q</sub> protein (B), G<sub>11</sub> protein (C), GRK2 (D), InsR (E), Akt2 (F) and GLUT4 (G) during differentiation of myoblasts into myotubes for 7 days. Semiquantitative RT-PCR experiments were carried out using total RNA prepared from 5 individual cell populations. Ordinate represents relative expression levels at Day 7 against Day 0. Data are presented as means ± SEM of the results obtained from 5 experiments. \**P* < 0.05, \*\**P* < 0.01, significantly different from unity.

**Figure S2** ET-1 induces phosphorylation of ERK1/2 but not Akt in L6 myotubes. The cells were treated with 30 nM ET-1 for indicated times. Representative immunoblots were obtained using antibodies to phospho-Akt at Thr<sup>308</sup> [p-Akt (T308)], phospho-Akt at Ser<sup>473</sup> [p-Akt (S473)], total Akt (t-Akt), phospho-ERK1/2 (p-ERK1/2), and total ERK1/2 (t-ERK1/2).

**Figure S3** No interaction of endogenous IRS-1 with FLAG-GRK2 is detected in L6 myotubes. Upper panel for immunoprecipitated samples (IP: α-normal IgG or FLAG): FLAG-tagged GRK2 proteins were immunoprecipitated with anti-FLAG antibody. Immunoprecipitates were probed with the anti-IRS-1 antibody to estimate co-immunoprecipitated endogenous IRS-1. Lower panel for IP: FLAG-tagged GRK2 proteins were immunoprecipitated with anti-FLAG antibody, and the immunoprecipitates were probed with the anti-FLAG-HRP antibody to normalize the quantity of co-immunoprecipitated endogenous Akt. Upper panel for whole cell lysate (WCL): the expressed IRS-1 was detected with the anti-IRS-1 antibody. Lower panel for WCL: the expressed FLAG-GRK2 was detected with the anti-FLAG-HRP antibody.

**Figure S4** Effects of YM-254890 on Akt phosphorylation in response to 5 min exposure to 300 nM insulin in L6 myotubes. The cells were treated with 300 nM YM-254890 for 30 min before stimulation with insulin. Representative immunoblots were obtained using antibodies to phospho-Akt at Thr<sup>308</sup> [p-Akt (T308)], phospho-Akt at Ser<sup>473</sup> [p-Akt (S473)], and total Akt (t-Akt). Ordinate represents Akt phosphorylation responses which are normalized to the level of insulin-stimulated Akt phosphorylation in L6 myotubes without treatment with YM-254890. Data are presented as means ± SEM of the results obtained from 5 experiments. Supplementary METHODS. Measurement of mRNA expression levels for ET<sub>A</sub> receptors, G<sub>q</sub> protein, G<sub>11</sub> protein, GRK2, InsR, Akt2 and GLUT4 by semiquantitative RT-PCR. Supplementary Movie S1. Spontaneous contraction of L6 myotubes (Day 7).